

Impact of intensified Indian Ocean winds on mesoscale variability in the Agulhas system

Björn C. Backeberg^{1,2*}, Pierrick Penven^{3,2} and Mathieu Rouault^{1,2}

South of Africa, the Agulhas Current retroflects and a portion of its waters flows into the South Atlantic Ocean¹, typically in the form of Agulhas rings². This flux of warm and salty water from the Indian to the Atlantic Ocean (the Agulhas leakage) is now recognized as a key element in global climate³. An Agulhas leakage shutdown has been associated with extreme glacial periods⁴, whereas a vigorous increase has preceded shifts towards interglacials⁵. In the absence of a coherent observing system, studies of the Agulhas have relied heavily on ocean models, which have revealed a possible recent increase in Agulhas leakage^{6–8}. However, owing to the high levels of oceanic turbulence, model solutions of the region are highly sensitive to their numerical choices^{9,10}, stressing the need for observations to confirm these important model results. Here, using satellite altimetry observations from 1993 to 2009, we show that the mesoscale variability of the Agulhas system, in particular in the Mozambique Channel and south of Madagascar, has intensified. This seems to result from an increased South Equatorial Current driven by enhanced trade winds over the tropical Indian Ocean. Overall, the intensified mesoscale variability of the Agulhas system is reflected in accelerated eddy propagation, in its source regions as well as the retroflexion from which eddies propagate into the South Atlantic Ocean. This suggests that the Agulhas leakage may have increased from 1993 to 2009, confirming previous modelling studies that have further implied an increased Agulhas leakage may compensate a deceleration of meridional overturning circulation associated with a freshening of the North Atlantic Ocean^{6,11}.

On a global scale, sea level rise is not geographically uniform^{12,13}. Figure 1a presents the decadal trend of sea surface height (SSH) in the Indian Ocean for the period 1993–2009.

An increase reaching 5 cm per decade is evident between 8° and 30° S east of Madagascar, whereas there is a marked decrease in the north. South of 30° S the pattern is less clear, showing a tendency towards a negative trend between 30° and 40° S and an increase between 40° and 45° S. This large-scale pattern is evident in the zonal mean from 15° to 120° E (Fig. 1b).

Mean SSH contours are overlaid to help analyse regional changes with respect to major surface currents (Fig. 1a). East of 100° E, SSH has increased by 2 cm per decade in the Indonesian Throughflow region. A strong positive trend, reaching 4 cm per decade, is centred near 10° S, between 70° and 100° E, in the core of the South Equatorial Current. North of the South Equatorial Current and the North Madagascar Current from the African coast to 70° E, a decreasing trend of 3 cm per decade is observed. A striking feature

is the large increase (5 cm per decade) within the gyre (12°–30° S, 40°–80° E) that is associated with the North Madagascar Current and the East Madagascar Current. This positive trend extends from south of Madagascar to the Agulhas Current. The pattern is more complex in the Agulhas Current region, with a decrease along the South African south and east coasts (20°–30° S) and a general increase downstream of the Agulhas retroflexion and in the Agulhas Return Current between 35°–45° S and 20°–75° E.

The geostrophic approximation leads to a simple relationship between ocean currents and the slope of the sea surface: SSH gradients are proportional to surface geostrophic currents. Considering the geostrophic circulation associated with the observed changes in SSH gradients, Fig. 1a,b suggests a general increase in surface currents within the western subtropical Indian Ocean, particularly between 50°–75° E and 8°–30° S, with an enhanced pressure gradient north of Madagascar and an intensified anticyclonic gyre east and south of Madagascar. Figure 1c presents the SSH trend derived from the Sverdrup relation, which provides the large-scale oceanic response to the curl of the wind stress exerted on the ocean surface. With the exception of the eastern Indian Ocean, the SSH changes evident in Fig. 1c are related to the zonally averaged wind-stress curl trend (Fig. 1d) and conform to the observed intensification of circulation east of Madagascar, between 8° and 30° S (Fig. 1a), in response to an increase in wind-stress curl at these latitudes (Fig. 1d). This increase in wind-stress curl is mainly due to an increase in trade winds^{8,12} (Fig. 2). From 1993 to 2009, the westerly winds have increased between 40°–50° S and 50°–90° E. Reanalysis products disagree over the changes in the westerlies from 1993 to 2009 (Supplementary Fig. S1), highlighting the need for consistent observations in the Southern Ocean.

The intensified westerly winds, combined with increased trade winds (Fig. 2) should result in a general increase in wind-stress curl over the Indian Ocean. Although there is no gyre-wide trend in the wind-stress curl, its increase is evident between 16° and 30° S (Fig. 1d). Comparing the observed (Fig. 1a) and wind-forced (Fig. 1c) trends in SSH confirms that long-term SSH changes in the core of the South Equatorial Current are associated with the winds over the Indian Ocean (Figs 1d and 2).

The increased large-scale circulation and pressure gradients are reflected in surface geostrophic velocities, particularly for the western side of the domain. In the mean kinetic energy (MKE) there is a large positive trend (exceeding 300 cm² s⁻² per decade) where the North Madagascar and South Equatorial currents join together north of the Mozambique Channel (Fig. 3a). Within the channel, circulation is dominated by mesoscale eddies¹⁴; the enhanced South Equatorial Current results in an increase in eddy kinetic energy

¹Nansen-Tutu Centre for Marine Environmental Research, University of Cape Town, 7701, South Africa, ²Department of Oceanography, MA-RE Institute, University of Cape Town, 7701, South Africa, ³LMI ICEMASA, Laboratoire de Physique des Océans, UMR 6523 (CNRS, IFREMER, IRD, UBO), 29280 Plouzané, France. *e-mail: bjorn.backeberg@nersc.no.

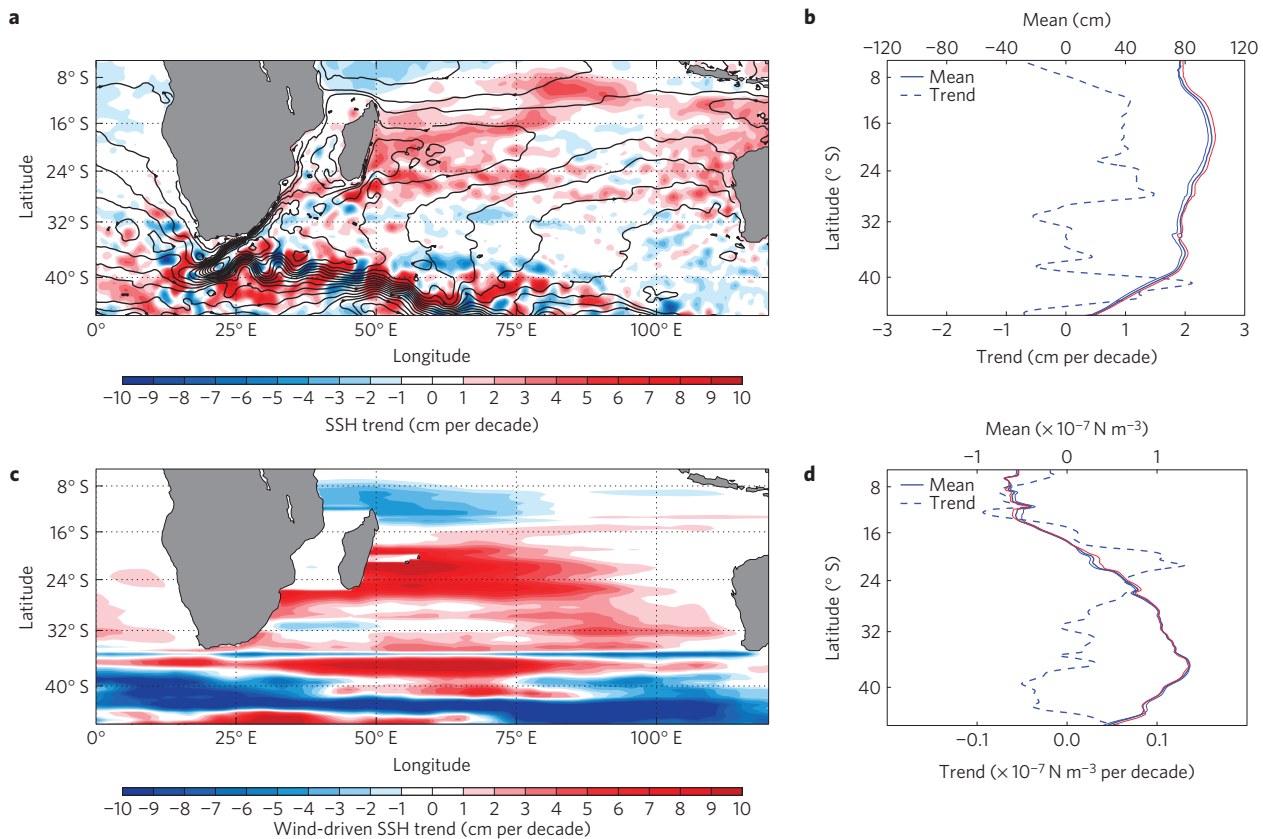


Figure 1 | Wind-driven intensification of the subtropical Indian Ocean gyre. **a**, Decadal trend of gridded SSH data from 1993 to 2009, a uniform global mean decadal trend of 3.4 cm per decade has been removed to account for the global sea level rise since 1993 (ref. 13). The black contours indicate the mean SSH for the period. **b**, Zonal mean SSH (solid line) and trend (dashed line) for 15°–120° E. The thin solid lines are the zonal mean SSH for 1993–1999 (blue) and 2003–2009 (red), illustrating the mean increase in SSH for the two periods. **c**, Decadal trend for 1993–2009 of the SSH derived from a Sverdrup relation forced by a wind-stress curl from CFSR (ref. 23) using an active layer of 200 m (ref. 26). **d**, Zonal mean wind-stress curl (solid line) and trend (dashed line) for 15°–120° E. The thin solid lines are the zonal mean wind-stress curl for 1993–1999 (blue) and 2003–2009 (red).

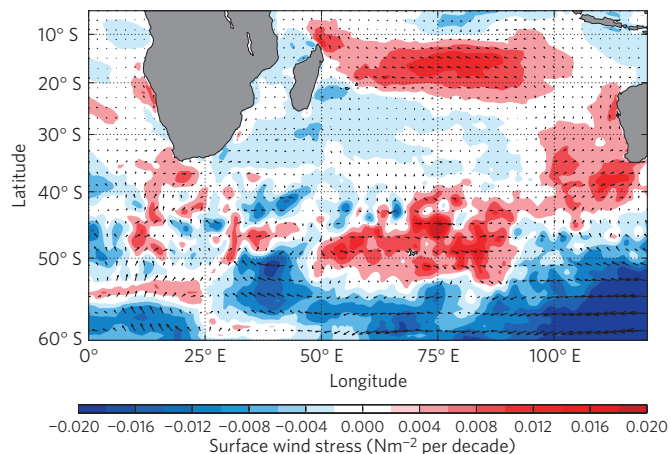


Figure 2 | Decadal trends of the surface wind stress of the subtropical Indian Ocean. Decadal trend of the surface wind-stress magnitude for 1993–2009 from the CFSR reanalysis²³ data. The vectors indicate the direction and magnitude of the trend.

(EKE), of up to 200 cm² s⁻² per decade (Fig. 3b). This is consistent with the connection between the South Equatorial Current north of Madagascar and the mesoscale variability in the Mozambique Channel¹⁵. For the region between 35°–48° E and 10°–20° S, the area-average EKE trend is 53 cm² s⁻² per decade (98% statistically significant). Eddy statistics show that this trend in EKE is associated

with a slight decrease in cyclone diameters and a doubling of the poleward propagation velocity of anticyclones (Table 1).

The southern branch of the East Madagascar Current also experiences an intensification of its mean flow component (Fig. 3a). At its southern extension, where high levels of mesoscale variability—associated with anticyclonic and cyclonic eddies—persist^{16,17}, the EKE shows strong positive trends (up to 240 cm² s⁻² per decade) extending from the southern tip of Madagascar towards the Agulhas Current (Fig. 3b). The area-average EKE trend for 40°–50° E and 27°–32° S is 75 cm² s⁻² per decade (98% statistically significant). The corresponding eddy statistics (Table 1) indicate that anticyclonic and cyclonic eddies increase in both amplitude and radii. The large increase in the westward propagation velocities of the cyclones is consistent with an increase in circulation.

Mesoscale features originating at the southern extension of the East Madagascar Current have been documented as an important contributor to the Agulhas system¹⁷. Increasing eddy properties (amplitudes, radii and westward propagation velocities) south of Madagascar imply increased volume transport towards the Agulhas system. Both the flow from the Mozambique Channel and the southern extension of the East Madagascar Current are considered to be important sources for the Agulhas Current^{16,18}. The intensification of the mean flow and its mesoscale variability may have downstream implications for the Agulhas Current and could influence the leakage into the South Atlantic Ocean.

In the Agulhas Current, the pattern of trends is more complex. The SSH trend shows an amplification of the circulation between the southern tip of Madagascar and the African coast (Fig. 1a). This

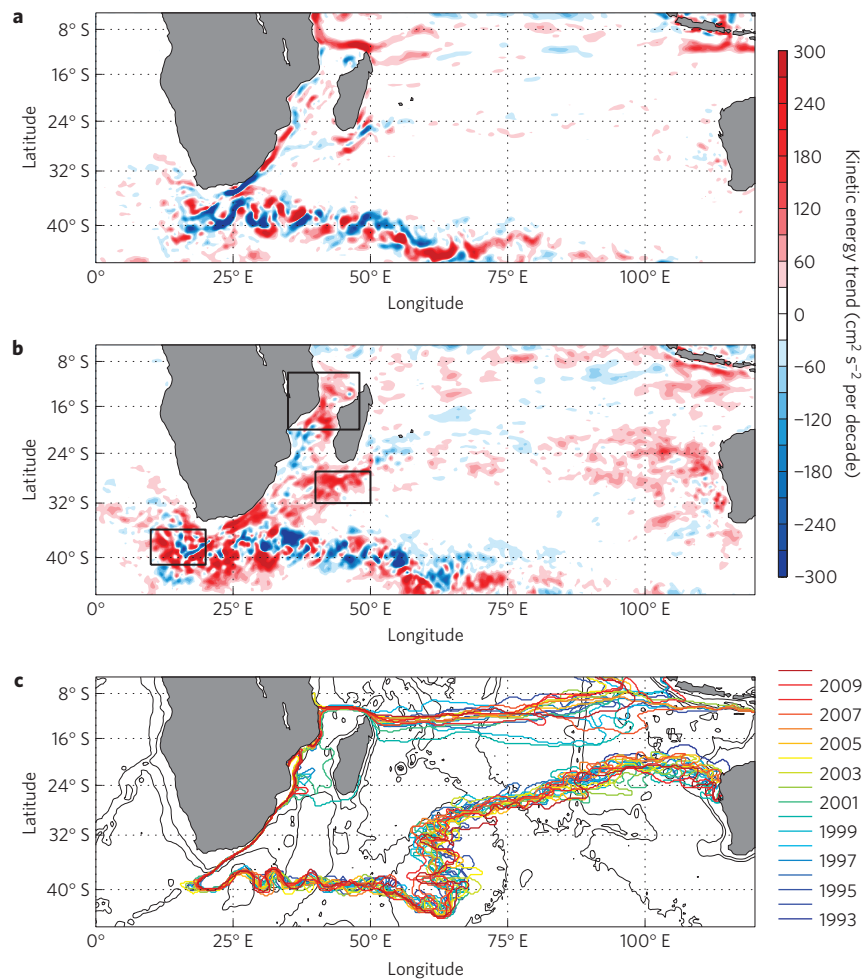


Figure 3 | Intensification of MKE and EKE. **a**, Decadal trend of the MKE calculated from absolute geostrophic velocities derived from altimetry SSH measurements for the period 1993–2009. **b**, The corresponding decadal trend of the EKE for the same period, the black boxes outline the areas for which the eddy statistics (Table 1) were generated using the eddy-detection scheme. **c**, Illustration of the interannual variations of the subtropical Indian Ocean gyre: streamlines of constant annual mean SSH from satellite altimetry traced from the inshore edge of the Agulhas Current (between the isobaths 200–1,000 m in the region 28°–32.5° E and 28°–32.5° S) over the entire subtropical Indian Ocean.

Table 1 | Eddy properties in the Agulhas system.

	MZC			SEMC			AR		
	Mean	Trend	<i>p</i>	Mean	Trend	<i>p</i>	Mean	Trend	<i>p</i>
Anticyclonic eddies									
Amplitude (cm)	12*	0.26*	0.62*	12	1.4	0.06	26*	0.58*	0.79*
Radius (km)	84	−2.4	0.17	67	3.0	0.18	66	0.88	0.30
<i>u</i> (cm s ^{−1})	−4.0*	−0.01*	0.89*	−3.8*	−0.04*	0.89*	−2.8	0.83	0.35
<i>v</i> (cm s ^{−1})	−2.0	−1.3	0.08	−0.2	−0.02	0.39	0.92	0.71	0.04
Cyclonic eddies									
Amplitude (cm)	11	−1.0	0.12	11	1.9	0.01	18	1.3	0.15
Radius (km)	75	−2.4	0.05	65	2.1	0.08	58	0.66	0.49
<i>u</i> (cm s ^{−1})	−4.2*	0.1*	0.95*	−4.2	−1.1	0.01	−2.1	0.58	0.32
<i>v</i> (cm s ^{−1})	−0.66	−0.59	0.34	−1.2*	−0.08*	0.69*	−0.12*	−0.4*	0.57*

Eddy statistics derived from the eddy-detection scheme for the Mozambique Channel (MZC), the southern extension of the East Madagascar Current (SEMC) and the Agulhas retroflection (AR) region. The mean amplitude, radius, *u* and *v* velocities of the eddy tracks as well as the corresponding decadal trends (unit/10 y) and the *p* value based on a two-tailed Spearman's rank correlation coefficient with 17 degrees of freedom are given for (a) anticyclonic and (b) cyclonic eddies. Values in bold correspond to *p* values below 0.1. *Correspond to insignificant trends.

is consistent with an increase in MKE of the northern Agulhas Current (from 32° S to 24° S, Fig. 3a). The connection between the Agulhas Current and its source regions is evident for the

southern extension of the East Madagascar Current in the EKE trend (Fig. 3b), with a positive trend extending from the southern tip of Madagascar towards the Agulhas Current (32°–26° S). On

reaching the African coast, the westward-propagating eddy energy is converted into MKE, which shows a positive trend in the northern Agulhas Current.

In contrast to the northern Agulhas Current, the MKE component of the southern Agulhas Current (32°–36° S; Fig. 3a) shows a decreasing trend, accompanied by a positive EKE trend (Fig. 3b). Eddy statistics for the region (22°–33° E, 30°–37° S) indicate increased westward and southward propagation velocities of anticyclonic eddies. Mean zonal and meridional eddy propagation velocities of -3.5 and -1.8 cm s^{-1} increase southwestward by 0.59 and 0.92 cm s^{-1} per decade, respectively ($p_{u\text{-trend}} = 0.14$ and $p_{v\text{-trend}} = 0.04$). The decreasing MKE and increasing EKE trends in the region imply that the energy contained in the current has shifted from the mean to the eddying component since 1993. This suggests that the southern Agulhas Current has become more variable. Moreover, intensified eddy-propagation velocities near the core of the Agulhas Current, its source regions and in the retroflexion, suggest that mesoscale variability in these three regions may be connected. However, it cannot be concluded that upstream changes directly impact the Agulhas retroflexion and leakage.

The increasing trend in EKE is also clearly evident in the Agulhas retroflexion region (Fig. 3b). The area-averaged trend for the retroflexion between 10°–20° E and 36°–41° S is $90 \text{ cm}^2 \text{ s}^{-2}$ per decade (90% statistical significance). Furthermore, the equatorward propagation velocity of the anticyclonic eddies has more than doubled (Table 1), indicating an enhanced intrusion of Agulhas rings into the Atlantic Ocean.

The above results indicate that the South Equatorial Current has intensified over the past 17 years in response to an increased wind-stress curl owing to an intensification of the Indian Ocean trade winds. The zonally averaged wind-stress curl east of Madagascar from 16° to 32° S shows trends of up to $0.125 \times 10^{-7} \text{ N m}^{-3}$ per decade. These trends are associated with intensified trade winds in the Indian Ocean¹⁹. The origin of the increased trade winds may be related to an enhanced Indian Ocean atmospheric Hadley circulation associated with increased sea surface temperatures and rainfall in the Indo-Pacific warm pool^{12,20}. This results in stronger pressure gradients between the tropics and the subtropics⁸.

The wind-induced intensification of the South Equatorial Current from 1993 to 2009 has caused the mean flow in the northern and southern branches of the East Madagascar Current to increase. This has affected the eddies observed in the Mozambique Channel and south of Madagascar, as is evident from the positive EKE trends in the region. In both cases, eddies move towards the Agulhas at increased rates, transporting more water towards the current (Table 1). The maximum eddy-rotation speed is larger than its translation velocity for more than 98% of the detected vortices, confirming their ability to transport material²¹. As the other eddy properties remain largely unchanged, this faster propagation could be caused by an increased background flow. In the northern Agulhas Current, the enhanced eddy energy from the Agulhas source regions is transferred into an intensified mean flow, whereas the southern Agulhas Current has shifted towards a more turbulent state. In general, an increase in the gyre circulation would enhance the potential for both barotropic and baroclinic instabilities.

Considering that the Indo-Atlantic leakage of warm, saline water occurs mainly through nonlinear mesoscale dynamics², an increased EKE in the Agulhas retroflexion region and an accelerated northward propagation of anticyclones implies that the Agulhas leakage may have increased over the past 17 years. This, in agreement with previous modelling studies, is further supported by an increasing trend (although not significant) in anticyclonic and cyclonic eddy radii (Table 1). Interestingly, this suggests that the Agulhas leakage seems to have increased despite a localized intensification of the westerlies over the retroflexion region.

Although there is evidence of increased mean circulation and increased mesoscale variability throughout the Agulhas system, including increased Agulhas leakage from accelerated Agulhas ring propagation, there is no indication that the mean position of the Agulhas retroflexion has changed from 1993 to 2009 (ref. 22). The annual mean positions of the gyre, observed by tracing altimetry SSH isolines from the inshore edge of the Agulhas Current over the entire gyre (Fig. 3c), show that the southern boundary of the gyre and the position of the retroflexion are remarkably stable on interannual scales. The decreasing MKE trend in the Agulhas retroflexion (10°–20° E, 36°–41° S) is weak and not significant: $-10 \text{ cm}^2 \text{ s}^{-2}$ per decade ($p = 0.67$), in contrast to the significant EKE trend for the area ($90 \text{ cm}^2 \text{ s}^{-2}$ per decade, $p = 0.06$). This indicates that the mean flow has not changed, despite the intensified mesoscale variability. The accelerated equatorward propagation of anticyclonic eddies into the South Atlantic, combined with a stable mean position of the Agulhas retroflexion²² (Fig. 3c), suggests that the location of the Agulhas retroflexion is not necessarily associated with a more energetic Agulhas Current system, nor an increased leakage.

Here we have shown that the mesoscale variability of the Agulhas system—in particular its source regions—has intensified from 1993 to 2009, owing to an increased South Equatorial Current. By combining altimetry observations with analyses of a temporally consistent wind reanalysis product²³, it was shown that these changes are driven by intensified trade winds over the tropical Indian Ocean. These results are further supported by recent publications documenting global and regional changes in sea level and intensified winds^{12,13,19,20}. Finally, effects on the eddies have been quantified using an eddy-tracking scheme, showing that enhanced mesoscale variability is reflected in accelerated eddy propagation throughout the Agulhas system. In the retroflexion, from which eddies propagate into the South Atlantic Ocean, this suggests that the Agulhas leakage may have increased from 1993 to 2009, confirming previous modelling results^{6–8}.

Methods

This work is based on the homogenous gridded absolute dynamic SSH topography data obtained from Aviso. SSH is obtained by combining measured sea level anomaly data from satellites with the Rio09 (ref. 24) mean dynamic topography, which has been shown to provide better estimates of the geostrophic velocities for the Agulhas Current²⁵. The zonal (u) and meridional (v) components of the geostrophic velocities are derived from SSH by $u = -g/f\eta_y$ and $v = g/f\eta_x$ and where g is gravity, f the Coriolis parameter and η the SSH.

MKE and EKE were calculated from SSH-derived geostrophic velocities. EKE is defined as $(\bar{u}^2 + \bar{v}^2)/2$, where $\bar{u}' = u - \bar{u}$ and $\bar{v}' = v - \bar{v}$; \bar{u} and \bar{v} being the annual mean for each individual year. MKE is defined as $(\bar{u}^2 + \bar{v}^2)/2$.

To illustrate the change in the wind-driven circulation, the barotropic transport is calculated from the Climate Forecast System Reanalysis (CFSR, ref. 23) wind-stress curl using the Sverdrup relation $V = (\nabla \times \tau)/(\beta\rho)$ where β is the rate of change of the Coriolis parameter with meridional distance, V is the vertically integrated meridional transport, τ the wind-stress vector and ρ the density of sea water. Using an active layer of 200 m (ref. 26)—extending from the ocean surface to the top of the thermocline, defined as the depth of the 17 °C isotherm at 32° S (ref. 27)—the associated SSH is derived.

All decadal trends are calculated using a least squares polynomial fit that minimizes the squared error. From the altimetry SSH trend, a uniform global mean sea level rise of 3.4 cm per decade, accounted for by ocean thermal expansion and land-ice melt¹³, has been removed. Statistical significance of the trends are based on a two-tailed Spearman's rank correlation coefficient with 17 degrees of freedom.

To quantify the relationship between the observed EKE to eddy changes, an eddy-detection scheme, combining the Okubo–Weiss and closed-contour methods²⁸, was implemented for key regions in the Agulhas system (where oceanic turbulence is the highest, see black boxes in Fig. 3b). An evaluation of different eddy detection methods is given in ref. 28. Here the detection is improved by combining two methods, reducing the sensitivity to the choice of parameters (for example, an Okubo–Weiss threshold²⁸), resulting in a more robust eddy detection. The eddy-tracking algorithm follows eddies by minimizing a generalized distance in parameter space from one frame to the subsequent frame^{26,28}. The statistics are presented in Table 1.

Received 13 September 2011; accepted 15 May 2012;
published online 8 July 2012

References

- Lutjeharms, J. R. E. *The Agulhas Current* (Springer-Praxis Books, 2006).
- Boebel, O. *et al.* The Cape Coudron: A regime of turbulent inter-ocean exchange. *Deep Sea Res. II* **50**, 57–86 (2003).
- Beal, L. M. *et al.* On the role of the Agulhas system in ocean circulation and climate. *Nature* **472**, 429–436 (2011).
- Bard, E. & Rickaby, R. E. Migration of the subtropical front as a modulator of glacial climate. *Nature* **460**, 380–383 (2009).
- Peeters, F. J. C. *et al.* Vigorous exchange between the Indian and Atlantic oceans at the end of the past five glacial periods. *Nature* **430**, 661–665 (2004).
- Biastoch, A., Böning, C. W., Schwarzkopf, F. U. & Lutjeharms, J. R. E. Increase in Agulhas leakage due to poleward shift of Southern Hemisphere westerlies. *Nature* **462**, 495–498 (2009).
- Dong, S., Garzoli, S. & Baringer, M. The Role of inter-ocean exchanges on decadal variations of the meridional heat transport in the South Atlantic. *J. Phys. Oceanogr.* **41**, 1498–1511 (2011).
- Rouault, M., Penven, P. & Pohl, B. Warming in the Agulhas Current system since the 1980's. *Geophys. Res. Lett.* **36**, L12602 (2009).
- Barnier, B. *et al.* Impact of partial steps and momentum advection schemes in a global ocean circulation model at eddy permitting resolution. *Ocean Dynam.* **56**, 543–567 (2006).
- Backeberg, B. C., Bertino, L. & Johannessen, J. A. Evaluating two numerical advection schemes in HYCOM for eddy-resolving modelling of the Agulhas Current. *Ocean Sci.* **5**, 173–190 (2009).
- Weijer, W., de Ruijter, W. P. M. & Dijkstra, H. A. Stability of the Atlantic overturning circulation: Competition between Bering Strait freshwater flux and Agulhas heat and salt sources. *J. Phys. Oceanogr.* **31**, 2385–2402 (2001).
- Han, W. *et al.* Patterns of Indian Ocean sea-level change in a warming climate. *Nature Geosci.* **3**, 546–550 (2010).
- Cazenave, A. & Llovel, W. Contemporary sea level rise. *Annu. Rev. Mar. Sci.* **2**, 145–173 (2010).
- de Ruijter, W. P. M., Ridderinkhof, H., Lutjeharms, J. R. E., Schouten, M. W. & Veth, C. Observations of the flow in the Mozambique Channel. *Geophys. Res. Lett.* **29**, 1502–1504 (2002).
- Backeberg, B. C. & Reason, C. J. C. A connection between the South Equatorial Current north of Madagascar and Mozambique Channel eddies. *Geophys. Res. Lett.* **37**, L04604 (2010).
- de Ruijter, W. P. M. *et al.* Eddies and dipoles around South Madagascar: Formation, pathways and large-scale impact. *Deep. Sea Res.* **51**, 383–400 (2004).
- Siedler, G. *et al.* Modes of the southern extension of the East Madagascar Current. *J. Geophys. Res.* **114**, C01005 (2009).
- Schouten, M. W., de Ruijter, W. P. M. & van Leeuwen, P. J. Upstream control of Agulhas Ring shedding. *J. Geophys. Res.* **107**, 109–3120 (2002).
- Young, I. R., Zieger, S. & Babanin, A. V. Global trends in wind speed and wave height. *Science* **332**, 451–455 (2011).
- Williams, A. & Funk, C. A westward extension of the warm pool leads to a westward extension of the Walker circulation, drying eastern Africa. *Clim. Dynam.* **37**, 2417–2435 (2011).
- Chelton, D. B., Schlax, M. G. & Samelson, R. M. Global observations of nonlinear mesoscale eddies. *Prog. Oceanogr.* **91**, 167–216 (2011).
- Dencausse, G., Arhan, M. & Speich, S. Spatio-temporal characteristics of the Agulhas Current retroflection. *Deep Sea Res.* **57**, 1392–1405 (2010).
- Saha, S. *et al.* The NCEP Climate Forecast System Reanalysis. *Bull. Am. Meteorol. Soc.* **91**, 1015–1057 (2010).
- Rio, M.-H., Schaeffer, P., Moreaux, G., Lemoine, J.-M. & Bronner, E. A new Mean Dynamic Topography computed over the global ocean from GRACE data, altimetry and *in situ* measurements. *Poster Communication at OceanObs09 Symposium* (2009).
- Rouault, M. J., Mouche, A., Collard, F., Johannessen, J. A. & Chapron, B. Mapping the Agulhas Current from space: An assessment of ASAR surface current velocities. *J. Geophys. Res.* **115**, C10026 (2010).
- Penven, P., Echevin, V., Pasapera, J., Colas, F. & Tam, J. Average circulation, seasonal cycle, and mesoscale dynamics of the Peru Current system: A modelling approach. *J. Geophys. Res.* **110**, C10021 (2005).
- McDonagh, E. L., Bryden, H. L., King, B. A., Sanders, R. J., Cunningham, S. A. & Marsh, R. Decadal changes in the south Indian Ocean thermocline. *J. Clim.* **18**, 1575–1590 (2005).
- Souza, J. M. A. C., de Boyer Montégut, C. & Le Traon, P. Y. Comparison between three implementations of automatic identification algorithms for the quantification and characterization of mesoscale eddies in the South Atlantic Ocean. *Ocean Sci.* **7**, 317–334 (2011).

Acknowledgements

This work has been supported by the Nansen-Tutu Centre for Marine Environmental Research and the International Centre for Education, Marine and Atmospheric Sciences over Africa. M.R. thanks the African Centre for Earth System Science, Water Research Commission and the National Research Foundation for financial support. The altimeter products were produced by Ssalto/Duacs and distributed by Aviso, with support from Cnes (www.aviso.oceanobs.com/duacs/). The CFSR data were obtained from the Research Data Archive of the Computational and Information Systems Laboratory at the National Center for Atmospheric Research. We would like to thank B. Pohl for his advice on the Antarctic Oscillation.

Author contributions

B.C.B. initiated the study and together with P.P. collected and analysed the data. All authors interpreted the results and contributed towards writing the manuscript.

Additional information

The authors declare no competing financial interests. Supplementary information accompanies this paper on www.nature.com/natureclimatechange. Reprints and permissions information is available online at www.nature.com/reprints. Correspondence and requests for materials should be addressed to B.C.B.